Neurobiology of Disease 124 (2019) 152–162

Contents lists available at ScienceDirect

Neurobiology of Disease

journal homepage: www.elsevier.com/locate/ynbdi

Reduction of microglial progranulin does not exacerbate pathology or behavioral deficits in neuronal progranulin-insufficient mice

Andrew E. Arrant, Anthony J. Filiano, Aashka R. Patel, Madelyn Q. Hoffmann, Nicholas R. Boyle, Shreya N. Kashyap, Vincent C. Onyilo, Allen H. Young, Erik D. Roberson*

Departments of Neurology and Neurobiology, Center for Neurodegeneration and Experimental Therapeutics, Alzheimer's Disease Center, Evelyn F. McKnight Brain Institute, University of Alabama at Birmingham, Birmingham, AL, United States

ARTICLE INFO

Keywords:
Neuron
Microglia
Progranulin
Frontotemporal dementia
Neuronal ceroid lipofuscinosis
Pathology
Behavior
Lysosome

ABSTRACT

Loss-of-function mutations in progranulin (*GRN*), most of which cause progranulin haploinsufficiency, are a major autosomal dominant cause of frontotemporal dementia (FTD). Individuals with loss-of-function mutations on both *GRN* alleles develop neuronal ceroid lipofuscinosis (NCL), a lysosomal storage disorder. Progranulin is a secreted glycoprotein expressed by a variety of cell types throughout the body, including neurons and microglia in the brain. Understanding the relative importance of neuronal and microglial progranulin insufficiency in FTD pathogenesis may guide development of therapies. In this study, we used mouse models to investigate the role of neuronal and microglial progranulin insufficiency in the development of FTD-like pathology and behavioral deficits. $Grn^{-/-}$ mice model aspects of FTD and NCL, developing lipofuscinosis and gliosis throughout the brain, as well as deficits in social behavior. We have previously shown that selective depletion of neuronal progranulin disrupts social behavior, but does not produce lipofuscinosis or gliosis. We hypothesized that reduction of microglial progranulin would induce lipofuscinosis and gliosis, and exacerbate behavioral deficits, in neuronal progranulin-deficient mice. To test this hypothesis, we crossed $Grn^{fl/fl}$ mice with mice expressing Cre transgenes targeting neurons (*CaMKII*-Cre) and myeloid cells/microglia (*LysM*-Cre). *CaMKII*-Cre, which is expressed in forebrain excitatory neurons, reduced cortical progranulin protein levels by around 50%. *LysM*-Cre strongly reduced progranulin immunolabeling in many microglia, but did not reduce total brain progranulin levels, suggesting that, at least under resting conditions, microglia contribute less than neurons to overall brain progranulin levels. Mice with depletion of both neuronal and microglial progranulin failed to develop lipofuscinosis or gliosis, suggesting that progranulin from extracellular sources prevented pathology in cells targeted by the Cre transgenes. Reduction of microglial progranulin also did not exacerbate the social deficits of neuronal progranulin-insufficient mice. These results do not support the hypothesis of synergistic effects between progranulin-deficient neurons and microglia. Nearly complete progranulin deficiency appears to be required to induce lipofuscinosis and gliosis in mice, while partial progranulin insufficiency is sufficient to produce behavioral deficits.

1. Introduction

Loss-of-function mutations in progranulin (*GRN*) are a major cause of dominantly-inherited frontotemporal dementia (FTD), accounting for as much as 5% of all FTD cases and 25% of familial FTD (Baker et al., 2006; Cruts et al., 2006; Gass et al., 2006). Most of these disease-causing mutations produce progranulin haploinsufficiency through nonsense-mediated decay, while others disrupt progranulin secretion or protein processing (Baker et al., 2006; Cruts et al., 2006; Gass et al., 2006; Shankaran et al., 2008; Wang et al., 2010; Pinarbasi et al., 2018). In rare cases, individuals have been found with loss-of-function mutations on both *GRN* alleles (Smith et al., 2012; Almeida et al., 2016). Instead of FTD, these individuals develop the lysosomal storage disorder neuronal ceroid lipofuscinosis (NCL), which has an earlier onset than FTD, and causes seizures and retinal degeneration (Smith et al., 2012; Almeida et al., 2016). Based on these genetic data, roughly 50% loss of progranulin causes FTD and nearly complete loss of progranulin causes NCL. While severe lysosomal dysfunction is generally thought to

Abbreviations: FTD, frontotemporal dementia; NCL, neuronal ceroid lipofuscinosis; GFAP, glial fibrillary acidic protein; SCMAS, subunit C of mitochondrial ATP synthase

* Corresponding author at: 1825 University Ave. SHEL 1110, Birmingham, AL 35294, United States.
E-mail address: eroberson@uabmc.edu (E.D. Roberson).

https://doi.org/10.1016/j.nbd.2018.11.011
Received 9 October 2018; Received in revised form 8 November 2018; Accepted 14 November 2018
Available online 15 November 2018
0969-9961/

be the cause of NCL, the mechanism by which progranulin haploinsufficiency causes FTD remains unclear.

Progranulin has several functions that could be relevant to FTD pathogenesis in *GRN* mutation carriers. Progranulin is expressed by both neurons and microglia in the brain, and has effects on both cell types (Ryan et al., 2009; Petkau et al., 2010). Progranulin has neurotrophic effects, as it promotes neuronal survival and outgrowth of axons and dendrites (Van Damme et al., 2008; Ryan et al., 2009; Chitramuthu et al., 2010; Gass et al., 2012; De Muynck et al., 2013; Beel et al., 2017; Longhena et al., 2017). Progranulin has an anti-inflammatory effect in macrophages and microglia. Progranulin-deficient macrophages and microglia have hyper-inflammatory phenotypes, including increased expression of pro-inflammatory cytokines (Yin et al., 2010a; Martens et al., 2012; Jackman et al., 2013; Lui et al., 2016; Krabbe et al., 2017). Despite this increased expression of inflammatory cytokines, progranulin-deficient microglia also exhibit impaired phagocytosis and motility (Minami et al., 2014; Krabbe et al., 2017). Finally, progranulin is critical for maintaining proper lysosomal function in both neurons and microglia, perhaps by regulating the activity of lysosomal enzymes (Tanaka et al., 2013; Jian et al., 2016; Lui et al., 2016; Beel et al., 2017; Chang et al., 2017; Valdez et al., 2017; Zhou et al., 2017). It is likely that impairment of some or all of these functions are involved in FTD pathogenesis in *GRN* mutation carriers.

Mouse models have been employed to investigate how progranulin haploinsufficiency may cause disease. Heterozygous knockout of progranulin in mice, modeling the progranulin haploinsufficiency that causes FTD, produces deficits in social behavior and fear memory, as well as mild lysosomal abnormalities in the brain (Filiano et al., 2013; Arrant et al., 2016; Arrant et al., 2017; Evers et al., 2017; Arrant et al., 2018). Homozygous knockout of progranulin in mice produces many of the same behavioral abnormalities observed in $Grn^{+/-}$ mice, as well as robust lysosomal abnormalities, elevated levels of inflammatory cytokines, and pathology that models aspects of the pathology of FTD and NCL (Kayasuga et al., 2007; Yin et al., 2010b; Ghoshal et al., 2012; Martens et al., 2012; Filiano et al., 2013; Arrant et al., 2017; Evers et al., 2017; Klein et al., 2017; Krabbe et al., 2017; Ward et al., 2017; Arrant et al., 2018). Specifically, $Grn^{-/-}$ mice develop lipofuscinosis, microgliosis, and astrogliosis, and at advanced ages exhibit elevated phospho-TDP-43 in the thalamus (Ahmed et al., 2010; Wils et al., 2012; Filiano et al., 2013; Tanaka et al., 2014).

In efforts to understand the relative contributions of neuronal and microglial progranulin deficiency to these phenotypes, we and others have crossed $Grn^{fl/fl}$ mice with mice expressing Cre transgenes under cell-type specific promoters to selectively deplete neuronal or microglial progranulin. Selective depletion of neuronal progranulin using *CaMKII*-Cre or *Nestin*-Cre in $Grn^{fl/fl}$ mice produces most of the behavioral deficits observed in global $Grn^{+/-}$ and $Grn^{-/-}$ mice (Arrant et al., 2017), but fails to produce the lipofuscinosis or gliosis observed in global $Grn^{-/-}$ mice (Arrant et al., 2017; Petkau et al., 2017a). Depletion of neuronal progranulin with *Thy1*-Cre in $Grn^{fl/fl}$ mice also impairs recovery from axonal injury (Beel et al., 2017). Similarly, selective depletion of microglial progranulin with *Cx3Cr1*-Cre in $Grn^{fl/fl}$ mice produces an excessive grooming phenotype also observed in global $Grn^{-/-}$ mice (Krabbe et al., 2017), but depletion of microglial progranulin with *LysM*-Cre in $Grn^{fl/fl}$ mice fails to produce the lipofuscinosis, gliosis, or baseline inflammatory phenotype observed in global $Grn^{-/-}$ mice (Petkau et al., 2017b). Despite the lack of associated pathology, selective depletion of microglial progranulin disrupts microglial function, as microglia from *LysM*-Cre:$Grn^{fl/fl}$ mice exhibit impaired phagocytosis (Minami et al., 2014), microglia from *Cx3Cr1*-Cre:$Grn^{fl/fl}$ mice exhibit impaired motility (Krabbe et al., 2017), and microglia from *Cd11b*-Cre:$Grn^{fl/fl}$ mice exhibit exaggerated inflammatory responses and greater neuronal loss after treatment with the dopaminergic neurotoxin 1-methyl-4-phenyl-1,2,3,6-tetrahydropyridine (Martens et al., 2012).

As depletion of neither neuronal nor microglial progranulin is sufficient to reproduce the pathology of global $Grn^{-/-}$ mice, we tested whether selective reduction of progranulin from both cell types might be sufficient to cause lipofuscinosis and gliosis. We previously observed that depletion of neuronal progranulin with *CaMKII*-Cre reduces cortical progranulin mRNA by around 50%, which is sufficient to disrupt social behavior, but not to produce pathology (Arrant et al., 2017). To determine if reduction of microglial progranulin might exacerbate the phenotypes of *CaMKII*-Cre neuronal progranulin-insufficient mice, we crossed $Grn^{fl/fl}$ mice expressing *CaMKII*-Cre with $Grn^{fl/fl}$ mice expressing *LysM*-Cre. We then assessed social behaviors and compulsive grooming in these mice, aged them to 20–24 months, and measured lipofuscinosis and gliosis in Cre–, *CaMKII*-Cre+, *LysM*-Cre+, or *LysM*-Cre+:*CaMKII*-Cre+ littermates.

2. Materials and methods

2.1. Mice

$Grn^{fl/fl}$ mice with *loxp* sites flanking the entire coding region of the mouse *Grn* gene were generated and crossed onto a C57BL/6J background as described previously (Martens et al., 2012). These $Grn^{fl/fl}$ mice were subsequently bred to mice expressing Cre under *CaMKII* (Jackson Laboratory *Camk2a*-Cre T29-1) (Tsien et al., 1996) or *LysM* promoters (Jackson Laboratory B6.129P2 - $Lyz2^{tm1(cre)Ifo}$) (Clausen et al., 1999) on a congenic C57BL/6J background. Offspring from these pairings were bred again with $Grn^{fl/fl}$ mice to generate mice expressing *CaMKII*-Cre or *LysM*-Cre on a homozygous $Grn^{fl/fl}$ background. Mice from each Cre line were then crossed to generate mice expressing *CaMKII*-Cre, *LysM*-Cre, or both *CaMKII*-Cre and *LysM*-Cre. Cre– littermates from these pairings were used as controls. Both male and female mice were used for this study.

Mice were genotyped with primers specific to the *CaMKII*-Cre or *LysM*-Cre transgenes. *CaMKII*-Cre was detected with a forward primer targeting the *CaMKII* promoter (GATAAGGTGGCGGTGTGAT ATGCACA) and a reverse primer targeting the Cre transgene (CCG GACCGACGATGAAGCATGTT). Thus, a band was only detected in mice carrying the *CaMKII*-Cre transgene when PCR reactions were run on an agarose gel. *LysM*-Cre was detected by a protocol described by Jackson Laboratory (https://www2.jax.org/protocolsdb/f?p=116:5:0::NO:5:P5_MASTER_PROTOCOL_ID,P5_JRS_CODE:28518,004781). The Cre transgene in this mouse line is inserted after the transcriptional start site of one *Lyz2* allele (Clausen et al., 1999). Primers flanking the transcriptional start site of the *Lyz2* gene were used to detect the wild-type *Lyz2* allele (forward –TTACAGTCGGCCAGGCTGAC, reverse – CTTGGGCTGCCAGA ATTTCTC), and a second forward primer targeting the inserted Cre transgene (CCCAGAAATGCCAGATTACG) was used to generate a second PCR product with the same reverse primer. Therefore, PCR products from Cre– mice displayed only one band on an agarose gel, but PCR products from mice carrying the *LysM*-Cre transgene displayed two bands, one from the wild-type *Lyz2* allele, and one from the inserted Cre transgene. Tail clips from all mice were collected at weening and genotyped for both Cre transgenes. Genotype was confirmed on tail clips collected during euthanasia.

Mice were kept in our housing facility accredited by the Association for Assessment and Accreditation of Laboratory Animal Care. The mice were maintained on a 12:12 h light schedule, with lights on at 06:00 and off at 18:00. Mice had free access to food (Harlan #7917) and water throughout the study. All experiments were approved by the Institutional Animal Care and use Committee at the University of Alabama at Birmingham.

Mice were anesthetized for tissue collection with 100 mg/kg pentobarbital (Fatal Plus, Vortech Pharmaceuticals). Blood was collected by cardiac puncture as previously described (Arrant et al., 2015). Mice were transcardially perfused with 0.9% saline. Brains were then removed and bisected into hemibrains. The left hemibrains were post-

fixed for 48 h in 4% paraformaldehyde and stored in PBS prior to cryosectioning into 30 μm sections for immunostaining on a sliding microtome (Leica). The right hemibrains were immediately frozen on dry ice and stored until dissection and processing for progranulin ELISA.

2.2. Immunostaining

The following antibodies were used for immunostaining: progranulin (R&D systems #AF2557), Iba1 (Wako #019-19741), NeuN (Millipore Sigma #MAB377), subunit C of mitochondrial ATP synthase (SCMAS) (Abcam #EPR13907), GFAP (Dako #Z0334) and CD68 (Bio-Rad #MCA1957). 30 μm free-floating sections were immunostained by overnight incubation with primary antibodies as previously described (Palop et al., 2011). Markers of pathology (SCMAS, GFAP, CD68) and progranulin were detected with species-matched biotinylated secondary antibodies (Vector Laboratories) followed by incubation with avidin-biotin complex (Vectastain Elite, Vector Laboratories), and visualized by incubation with diaminobenzidene (MP Biomedicals). Progranulin immunolabeling of neurons and microglia was determined as previously described (Arrant et al., 2017) by sequential immunostaining for progranulin and markers of neurons (NeuN) and microglia (Iba1). Species-matched Alexa-fluor-488 or -594 secondary antibodies (ThermoFisher Scientific) were used to detect immunostaining.

Several approaches were used for immunostaining imaging and analysis. For quantitation, two images were taken per brain region per mouse and averaged to give a final value. ImageJ was used for image processing and analysis as described below. Qualitative scoring of progranulin immunoreactivity in microglia was performed as described previously (Arrant et al., 2017). Brain sections were co-stained with antibodies against progranulin and Iba1 and imaged with a Leica TCS-SP5 laser scanning confocal microscope. Maximum intensity projections were made for each channel and converted to binary images. Colocalization was determined using the "AND" function of the image calculator in ImageJ, and Iba1 + cells were qualitatively scored as having strong, punctate, or undetectable levels of progranulin immunolabeling. Regional progranulin immunostaining was assessed by densitometry of high resolution, low magnification scans (Pathscan Enabler IV, Meyer Instruments) of progranulin-immunostained brain sections, as described previously (Arrant et al., 2017). Lipofuscinosis and gliosis were assessed by measuring the percent area of pathology in 20× images, and c-Fos immunoreactivity was assessed by counting the number of immunoreactive cells in 4× images taken with an upright microscope (Nikon), as described previously (Arrant et al., 2017). Representative images of neuronal and microglial progranulin immunolabeling were obtained by co-staining brain sections for neuronal (NeuN) and microglial (Iba1) markers and imaging at 60× on a Nikon Ti2-C2 confocal microscope.

2.3. Progranulin ELISA

Progranulin levels in brain samples were determined by ELISA (Adipogen) using the manufacturer's protocol as previously described (Arrant et al., 2015). Brain samples were lysed in a mild NP-40 lysis buffer (10 mM Tris, 10 mM NaCl, 3 mM MgCl2-6H2O, 1 mM EDTA, 0.05% NP-40) and diluted 1:1 with ELISA buffer before analysis.

2.4. qPCR

Grn mRNA was measured by qPCR as described previously (Arrant et al., 2015). RNA was isolated from brain samples with Trizol (ThermoFisher), treated with DNase (DNA-free, ThermoFisher), and reverse transcribed into cDNA using Superscript III reverse transcriptase (ThermoFisher). *Grn* mRNA was detected using a Taqman probe (Mm01245914_g1, ThermoFisher) and normalized to levels of *Actb* (Mm00607939_s1, ThermoFisher).

2.5. Progranulin western blot

Levels of progranulin in plasma samples were assessed by western blot as described previously (Arrant et al., 2015). Plasma (2 μL) was diluted with LDS sample buffer (ThermoFisher) and Bolt sample reducing agent (ThermoFisher), and run on 4–12% Bis-Tris gels (ThermoFisher) before transferring to Immobilon-FL PVDF (MilliporeSigma). Progranulin was detected with an anti-mouse progranulin antibody (R&D Systems #AF2557), followed by a biotinylated anti-sheep secondary antibody (Vector Laboratories) and IR-Dye 800-labelled streptavidin (LI-COR Biosciences).

2.6. Amygdala activation in a novel, social environment

Amygdala activation in a novel, social environment was conducted as previously described (Scearce-Levie et al., 2008; Filiano et al., 2013). Two mice of the same genotype, but opposite sex, were placed in a novel cage with a variety of stimuli for two hours before transcardial perfusion with 0.9% saline. Brains were then immunostained for c-Fos as described above to assess neuronal activation.

2.7. Three-chamber sociability

The three-chamber sociability test was conducted as previously described (Filiano et al., 2013). Mice were allowed to freely explore a three-chambered testing apparatus for 10 min prior to the introduction of wire cages containing a novel mouse (adult male C57Bl/6J) or a novel object. Investigation of the novel mouse and object was then monitored for 10 min using video tracking software (Cleversys).

2.8. Grooming

Mice were placed in a clean cage with no bedding for 10 min, then placed in a recording chamber (Med Associates) and recorded with StereoScan software (Cleversys). Grooming was scored by an observer blind to mouse genotype as described previously (Warmus et al., 2014).

2.9. Tube test for social dominance

The tube test for social dominance was conducted as previously described (Arrant et al., 2016). Mice of the same sex, but opposite genotype, were released into opposite ends of a clear plastic tube and allowed to freely interact. Under these conditions, one mouse will force the other out of the tube. The first mouse with two feet out of the tube was considered to have lost the match. Each mouse was paired with three different opponents of the opposite genotype, and the winning percentage was calculated for each mouse by dividing the number of wins by the total number of matches.

2.10. Statistics

Levels of progranulin protein and RNA in *LysM*-Cre + mice, progranulin immunoreactivity in *LysM*-Cre:*CaMKII*-Cre + mice, c-Fos immunoreactivity, lipofuscin, SCMAS, GFAP, and CD68 were analyzed by repeated measures ANOVA with factors of *LysM*-Cre, *CaMKII*-Cre, and brain region. Levels of progranulin protein and RNA in individual brain regions of *LysM*-Cre:*CaMKII*-Cre + mice were analyzed by two-way ANOVA with factors of *LysM*-Cre and *CaMKII*-Cre, followed by Tukey's post-hoc test. Control $Grn^{-/-}$ pathology data were analyzed by repeated measures ANOVA followed by *t*-test for each brain region. Microglial progranulin immunolabeling was compared by Chi-square test. Plasma progranulin levels were analyzed by *t*-test. Winning percentage in the tube test for social dominance was analyzed by Mann-Whitney test. Sociability was analyzed by two-way ANOVA with factors of *LysM*-Cre and *CaMKII*-Cre, followed by Dunnett's post-hoc test. Grooming was analyzed by two-way repeated measures ANOVA

(factors of genotype and age) to compare *LysM*-Cre+, *CaMKII*-Cre+, and *LysM*-Cre:*CaMKII*-Cre + mice to Cre– mice. To correct for multiple comparisons on grooming behavior, p values were multiplied by 3. Two-tailed p values were calculated for all analyses, and α was set at 0.05. GraphPad Prism 7 was used for all analyses except for three-way repeated measured ANOVA of progranulin, lipofuscin, SCMAS, GFAP, and CD68, which was performed with SPSS 2.4. Data are presented as mean ± SEM.

3. Results

3.1. LysM-cre reduces microglial progranulin, but does not reduce total brain progranulin

To reduce progranulin levels in microglia, we crossed $Grn^{fl/fl}$ mice with mice expressing *LysM*-Cre (hereafter, the resulting *LysM*-Cre:$Grn^{fl/fl}$ mice are referred to as *LysM*-Cre + mice). *LysM*-Cre targets myeloid cells, and is expressed in monocytes, macrophages and neutrophils (Clausen et al., 1999; Abram et al., 2014). *LysM*-Cre has been reported to reduce microglial progranulin RNA levels by > 50% when expressed in $Grn^{fl/fl}$ mice (Minami et al., 2014; Petkau et al., 2017b). To assess microglial progranulin expression, we measured progranulin immunolabeling of microglia in the corpus callosum to avoid interference from neuronal progranulin. We confirmed that *LysM*-Cre + mice had reduced progranulin immunolabeling in most microglia (Fig. 1A, B). However, this reduction in microglial progranulin was not sufficient to significantly reduce total progranulin levels in the frontal cortex or thalamus (Fig. 1C, D), which is also consistent with prior data (Petkau et al., 2017b) and suggests that in vivo, microglia are not the predominant source of brain progranulin. As expected given its expression in peripheral myeloid cells, *LysM*-Cre reduced plasma progranulin levels by approximately 25% (Fig. 1E), showing that monocytes, macrophages, and neutrophils are a significant source of circulating progranulin.

3.2. Reduction of microglial progranulin does not cause lipofuscinosis, gliosis, or behavioral deficits

Before crossing *LysM*-Cre + microglial progranulin-insufficient mice with *CaMKII*-Cre+ neuronal progranulin-insufficient mice, we assessed whether reduction of microglial progranulin alone was sufficient to cause the pathology or behavioral deficits observed in global progranulin-insufficient mice. A small number of brains from global $Grn^{-/-}$ mice were run as positive controls, but not included in the statistical analysis. We found no elevation of autofluorescent lipofuscin (Fig. 2A), the astrocyte marker GFAP (Fig. 2B), or the microglial lysosomal protein CD68 (Fig. 2C) in brains of 12–13 month-old *LysM*-Cre + mice, showing that reduction of microglial progranulin does not produce the lipofuscinosis or microgliosis observed in global $Grn^{-/-}$ mice (Ahmed et al., 2010; Wils et al., 2012; Filiano et al., 2013; Tanaka et al., 2014).

In prior work, we found that global $Grn^{+/-}$ mice and neuronal progranulin-insufficient mice (*CamKII*-Cre + and *Nestin*-Cre +) have abnormally low social dominance and impaired amygdala activation during exposure to a novel, social environment, both of which develop by around 12 months of age (Filiano et al., 2013; Arrant et al., 2016; Arrant et al., 2017). We therefore tested *LysM*-Cre + microglial progranulin-insufficient mice in these assays at age 13–14 months, but observed no significant social dominance abnormalities (Fig. 2D). Microglial progranulin reduction also failed to significantly impair amygdala activation in a novel, social environment (Fig. 2E), although there was a clear trend for reduced activation in *LysM*-Cre + mice.

Together, the data from *LysM*-Cre + microglial progranulin-insufficient mice show that reduction of microglial progranulin is not sufficient to reduce total brain progranulin levels, induce lipofuscinosis and gliosis, or cause social dominance deficits like those in global progranulin-insufficient mice. While neuronal progranulin depletion induces greater functional deficits, akin to those in global progranulin-insufficient mice, it also fails to induce lipofuscinosis and gliosis (Arrant et al., 2017; Petkau et al., 2017a). This raises the possibility that

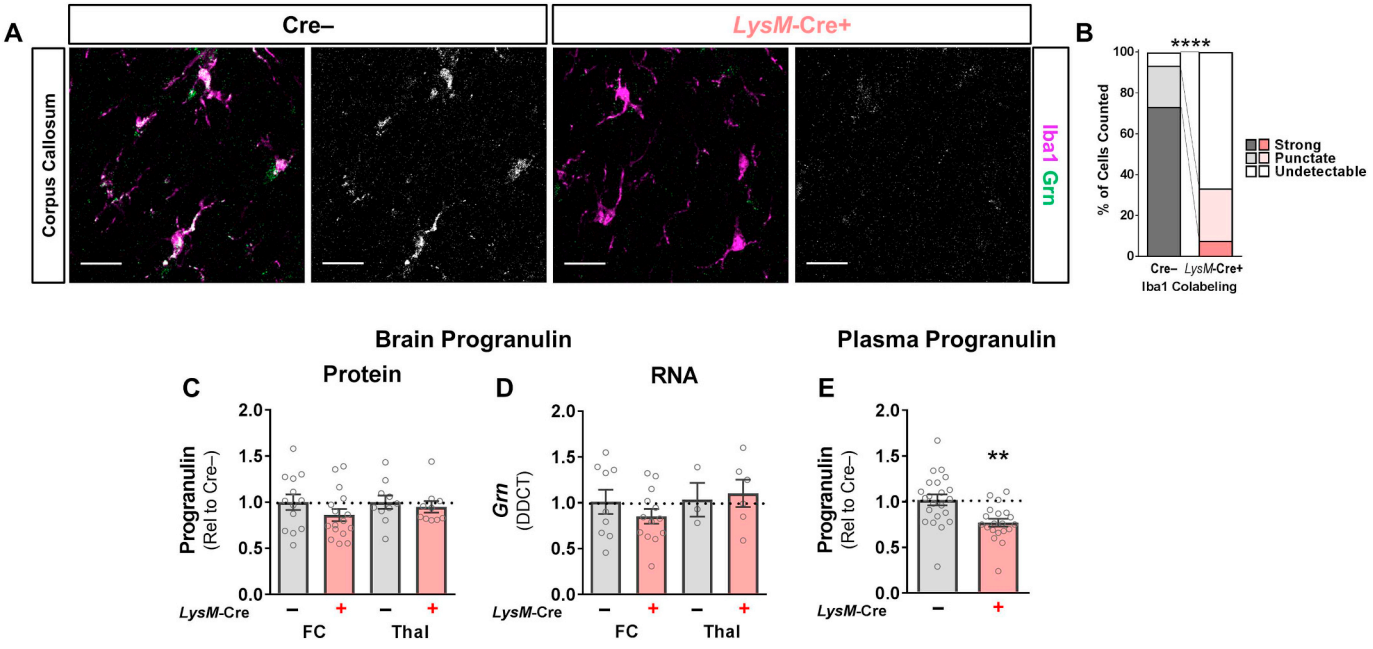

Fig. 1. *LysM*-Cre Reduces Microglial Progranulin, but Does Not Reduce Total Brain Progranulin.
LysM-Cre significantly reduced progranulin immunolabeling in microglia located in the corpus callosum (A, B, chi-square, $p < .0001$, $n = 398$ microglia from 5 Cre– mice and 285 microglia from 5 *LysM*-Cre + mice). However, *LysM*-Cre failed to significantly reduce total brain progranulin protein (C, ANOVA effect of *LysM*-Cre, $p = .2075$, $n = 10–17$ mice per group) or RNA (D, ANOVA effect of genotype, $p = .7602$, n = 3–13 mice per group). In contrast, *LysM*-Cre reduced plasma progranulin levels by around 25% (E, *t*-test, $p = .0019$, $n = 20–22$ mice per group). In A, progranulin immunostaining is shown in grayscale next to merged progranulin/Iba1 images. Scale bars in A represent 20 μm. FC = frontal cortex, Thal = thalamus. ** = $p < .01$ by *t*-test, **** = $p < .0001$ by Chi-square test.

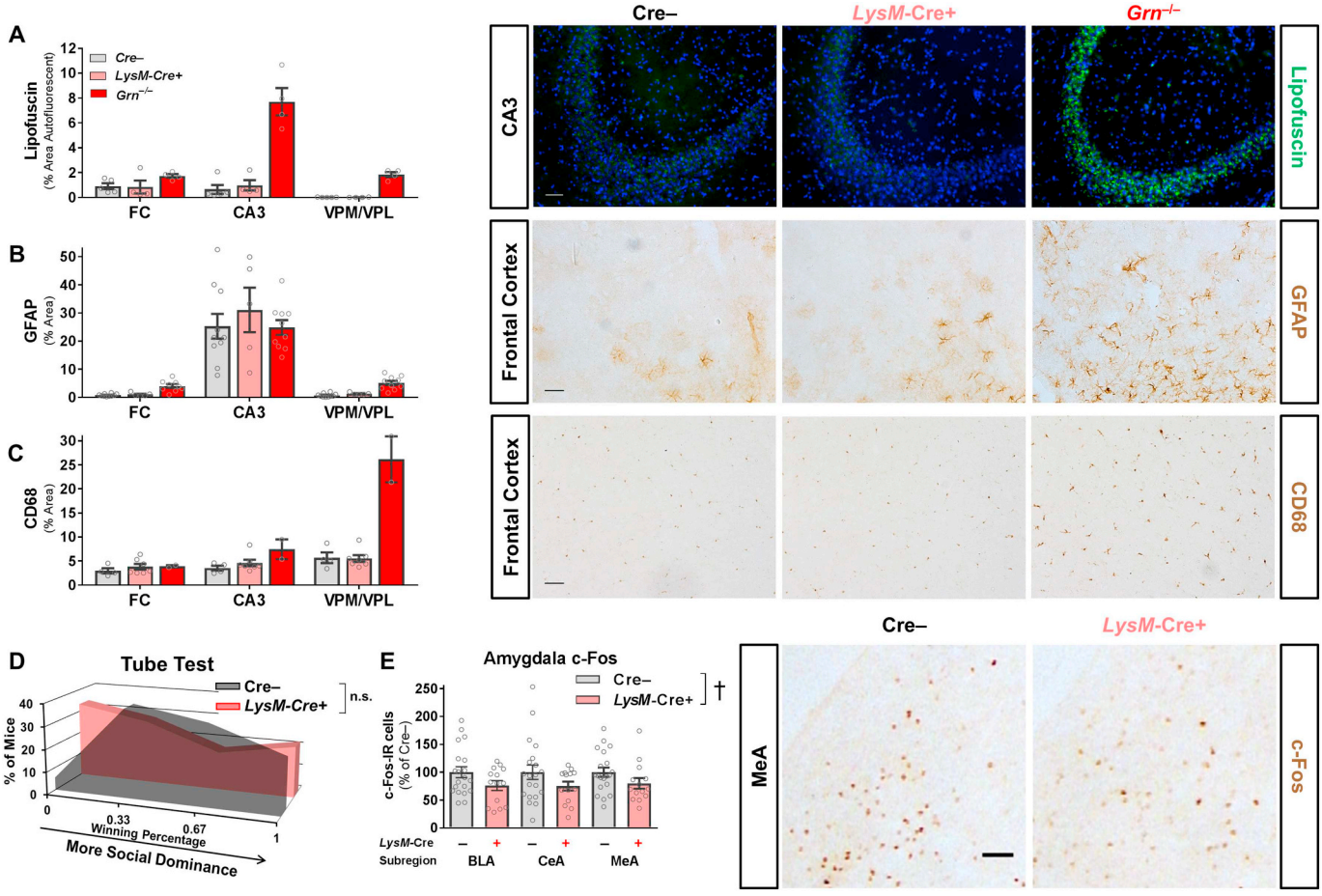

Fig. 2. Microglial Progranulin Reduction with *LysM*-Cre Does Not Produce Lipofuscinosis, Gliosis, or Social Dominance Deficits.
Microglial progranulin reduction with *LysM*-Cre in 12–13 month-old $Grn^{fl/fl}$ mice failed to produce the lipofuscinosis (A, RM ANOVA effect of *LysM*-Cre, $p = 7569$, $n = 4$–5 mice per group), astrogliosis (B, RM ANOVA effect of *LysM*-Cre, $p = .6618$, $n = 5$–10 mice per group), or microgliosis (C, RM ANOVA effect of *LysM*-Cre, $p = .6871$, n = 4–7 mice per group) that are typically observed in global $Grn^{-/-}$ mice. At age 13–14 months, microglial progranulin reduction also failed to produce the social dominance deficits (D, Mann-Whitney test, $p = .1931$, $n = 18$ mice per genotype) observed in global progranulin-insufficient mice and neuronal progranulin-insufficient mice. Microglial progranulin reduction also failed to significantly impair the amygdala response to a novel, social environment (E), though there was a clear trend (RM ANOVA effect of *LysM*-Cre, $p = .0627$, $n = 14$–20 mice per genotype) for less amygdala activation in *LysM*-Cre microglial progranulin-insufficient mice. Scale bars for lipofuscin, GFAP, and CD68 images represent 50 μm, the scale bar for c-Fos images represents 20 μm. VPM/VPL = ventroposteromedial/ventroposterolateral thalamus, BLA = basolateral amygdala, CeA = central amygdala, MeA = medial amygdala. † = $p < .1$.

development of lipofuscinosis and gliosis requires an interaction between progranulin-deficient neurons and progranulin-deficient microglia. To better understand the interaction of neuronal and microglial progranulin, we crossed *LysM*-Cre + microglial progranulin-insufficient mice with *CaMKII*-Cre + neuronal progranulin-insufficient mice.

3.3. Simultaneous expression of CaMKII-Cre and LysM-Cre reduces both neuronal and microglial progranulin

We previously confirmed that *CaMKII*-Cre reduces neuronal progranulin (Arrant et al., 2017), and observed that *LysM*-Cre reduces microglial progranulin (Fig. 1A, B). After crossing *LysM*-Cre + and *CaMKII*-Cre + mice, we performed immunostaining to confirm that *LysM*-Cre + :*CaMKII*-Cre + mice exhibited a reduction of both neuronal and microglial progranulin (Fig. 3A–D). We observed the expected reduction in progranulin immunolabeling of neurons (Fig. 3A, B), and microglia (Fig. 3C, D).

3.4. Reduction of microglial progranulin does not further reduce brain progranulin in neuronal progranulin-deficient mice

Despite the minimal impact of reducing microglial progranulin on total brain progranulin in *LysM*-Cre + microglial progranulin-insufficient mice (Fig. 1C, D), we hypothesized that reducing microglial progranulin might further reduce total brain progranulin in neuronal progranulin-insufficient mice. We previously observed that *CaMKII*-Cre reduces cortical progranulin mRNA levels by around 50% (Arrant et al., 2017), and therefore tested whether expression of *LysM*-Cre could further reduce progranulin levels in *CaMKII*-Cre + mice. We used progranulin immunostaining to screen progranulin levels throughout the forebrain, and observed the expected reduction in progranulin levels with *CaMKII*-Cre in the cortex, hippocampus, and basolateral amygdala (Fig. 3E). *LysM*-Cre had no effect on progranulin immunoreactivity, even in *CaMKII*-Cre + mice. To more quantitatively assess progranulin, we performed a progranulin ELISA on cortical and hippocampal tissue. Consistent with our prior data, mice expressing *CaMKII*-Cre exhibited an approximately 50% reduction in cortical progranulin levels and a 20–25% reduction in hippocampal progranulin levels (Fig. 3F, G). *LysM*-Cre + :*CaMKII*-Cre + mice expressing Cre in both microglia and neurons exhibited a nearly identical reduction of progranulin protein as mice expressing only *CaMKII*-Cre. Similarly, mice expressing *CaMKII*-Cre exhibited > 40% reduction of hippocampal *Grn* RNA levels (Fig. 3H). *LysM*-Cre + :*CaMKII*-Cre + mice failed to exhibit a significantly greater reduction in hippocampal *Grn* RNA than mice

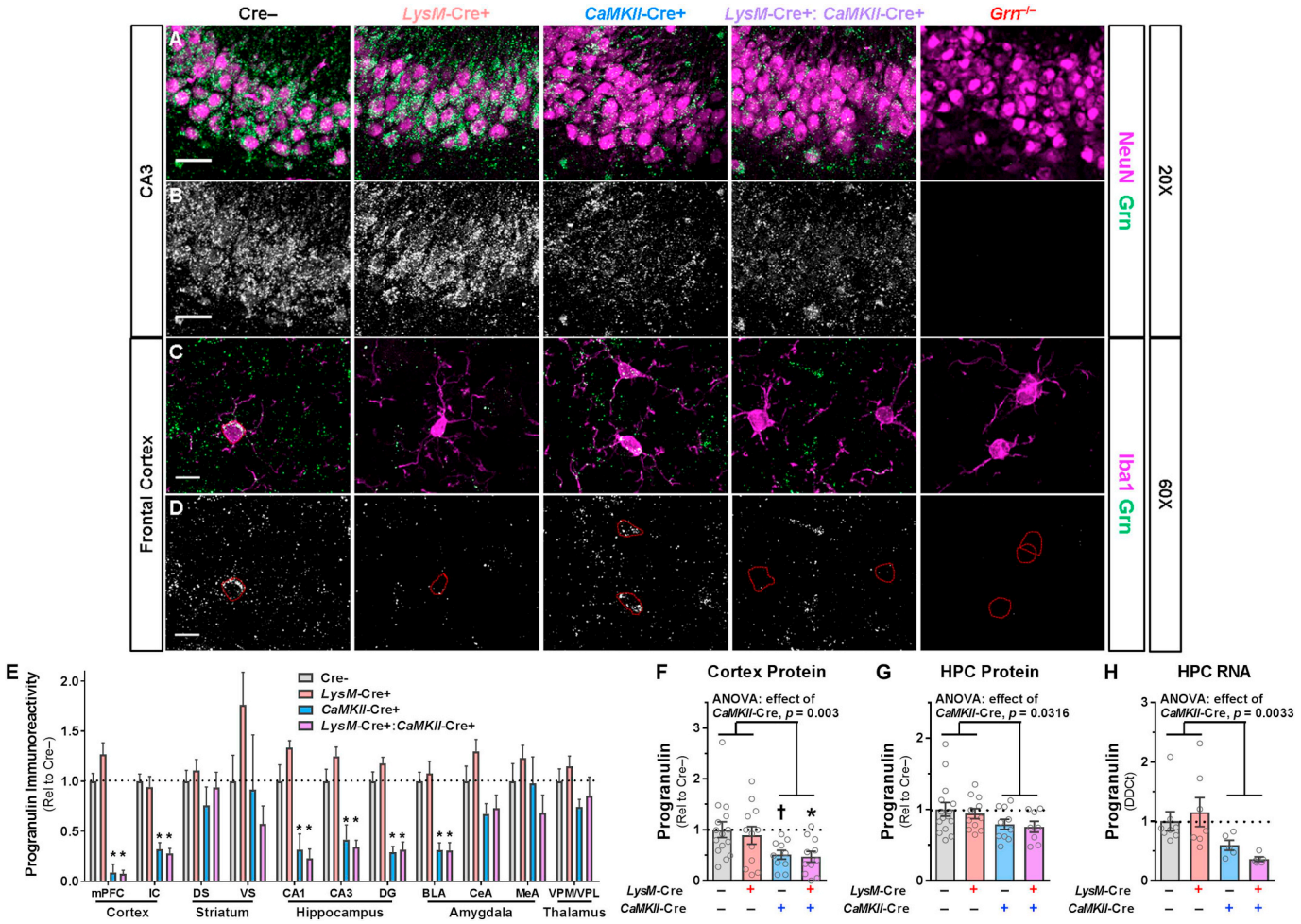

Fig. 3. *Grn*$^{fl/fl}$ Mice Expressing *LysM*-Cre and *CaMKII*-Cre Exhibit Reduction of Both Microglial and Neuronal Progranulin Immunoreactivity, but Only *CaMKII*-Cre Reduces Total Brain Progranulin.

Representative images showing progranulin immunolabeling of neurons (NeuN, A, B) and microglia (Iba1, C, D). The progranulin channel corresponding to double-labelled images is shown in B and D. *LysM*-Cre reduced microglial progranulin in *LysM*-Cre + and *LysM*-Cre + :*CaMKII*-Cre + mice, and *CaMKII*-Cre reduced neuronal progranulin in *CaMKII*-Cre + and *LysM*-Cre + :*CaMKII*-Cre + mice. Scale bars in A and B represent 30 μm and scale bars in C and D represent 10 μm. Outlines of microglial cell bodies are shown in red in D. Analysis of progranulin immunoreactivity in high resolution, low magnification scans of brain sections revealed that *CaMKII*-Cre, but not *LysM*-Cre, reduced total progranulin levels in the cortex, hippocampus, and basolateral amygdala (E, RM ANOVA effect of *CaMKII*-Cre, $p < .001$, *CaMKII*-Cre x region interaction, $p = .007$, n = 4–10 mice per group). Progranulin ELISA also showed that CaMKII-Cre reduced progranulin protein levels (RM ANOVA effect of *CaMKII*-Cre, $p = .002$), with cortical progranulin protein levels reduced by around 50% in mice expressing *CaMKII*-Cre (F, ANOVA effect of *CaMKII*-Cre, $p = .003$, n = 10–15 mice per group), and hippocampal progranulin protein levels reduced by 20–25% in mice expressing *CaMKII*-Cre (G, ANOVA effect of *CaMKII*-Cre, $p = .0316$, $n = 8–15$ mice per group). *LysM*-Cre had no significant effect on progranulin in either brain region. Consistent with the reduction in progranulin protein levels, *CaMKII*-Cre also reduced progranulin RNA in the hippocampus (H, ANOVA effect of *CaMKII*-Cre, $p = .0033$, n = 5–8 mice per group), while *LysM*-Cre had no significant effect. *LysM*-Cre + :*CaMKII*-Cre + mice did not exhibit greater reduction in total progranulin levels than mice expressing only *CaMKII*-Cre in any measure of progranulin protein or RNA. mPFC = medial prefrontal cortex, IC = insular cortex, DS = dorsal striatum, VS = ventral striatum, DG = dentate gyrus, BLA = basolateral amygdala, CeA = central amygdala, MeA = medial amygdala, VPM/VPL = ventral posteromedial/ventral posterolateral thalamus, HPC = hippocampus. † = $p < .1$, and * = $p < .05$ by Tukey's post-hoc test.

expressing only *CaMKII*-Cre (Tukey's post-hoc test, $p = .835$). These data show that microglial progranulin reduction does not further reduce progranulin levels in neuronal progranulin-insufficient mice.

3.5. Reduction of both neuronal and microglial progranulin does not cause lipofuscinosis or microgliosis

We next tested whether reduction of both neuronal and microglial progranulin could replicate the lipofuscinosis of global *Grn*$^{-/-}$ mice and homozygous *GRN* mutation carriers (Ahmed et al., 2010; Smith et al., 2012; Wils et al., 2012; Filiano et al., 2013; Tanaka et al., 2014). For analysis of pathology, we aged a cohort of Cre–, *LysM*-Cre +, *CaMKII*-Cre +, and *LysM*-Cre + :*CaMKII*-Cre + littermates to 22–24 months. As a positive control, we analyzed brain sections from 7 to 10 month-old *Grn*$^{-/-}$ mice. As expected, *Grn*$^{-/-}$ mice exhibited robust lipofuscinosis (Fig. 4A–D) and increased levels of subunit C of mitochondrial ATP synthase (SCMAS, Fig. 4E–H), a characteristic protein component of lipofuscin (Hall et al., 1991; Kominami et al., 1992). We observed no significant effect of *LysM*-Cre or *CaMKII*-Cre, either alone or in combination, on accumulation of autofluorescent lipofuscin (Fig.4B–D), or SCMAS (Fig. 4F–H).

We also tested whether selective reduction of both neuronal and microglial progranulin could replicate the gliosis of global *Grn*$^{-/-}$ mice, also seen in FTD patients with *GRN* mutations, by measuring immunostaining for the astrocyte marker GFAP and the microglial lysosomal protein CD68 (Fig. 5). *Grn*$^{-/-}$ mice exhibited the expected increases in GFAP (Fig. 5A–D) and CD68 (Fig. 5E–H). Similar to the analysis of lipofuscinosis, we observed no significant effect of *LysM*-Cre

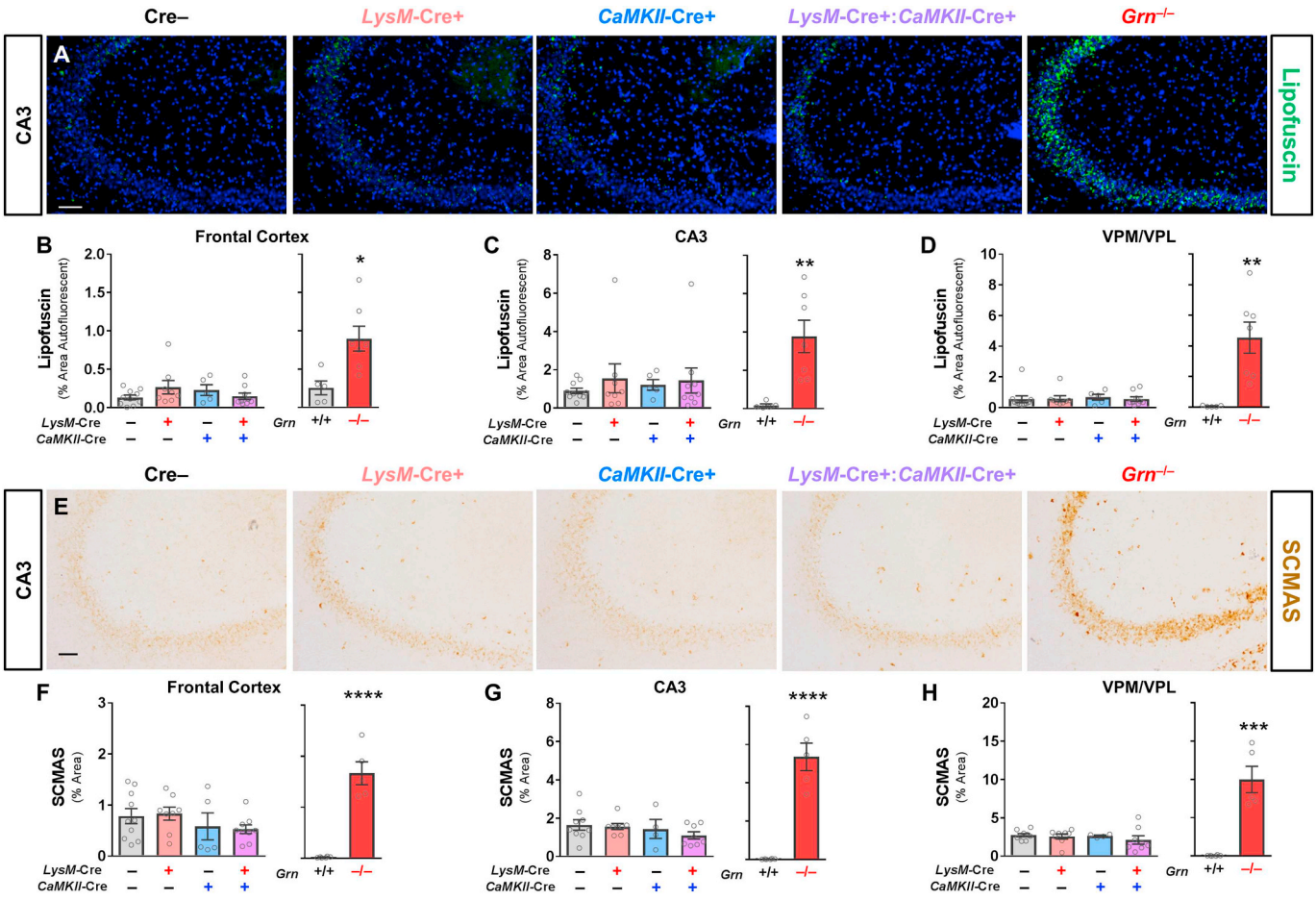

Fig. 4. Microglial Progranulin Reduction Does Not Produce Lipofuscinosis in *CaMKII*-Cre Neuronal Progranulin-insufficient Mice.
As expected, 7–10 month-old $Grn^{-/-}$ mice exhibited lipofuscinosis throughout the forebrain (A–D, RM ANOVA effect of genotype, $p = .0022$, n = 5–7 mice per group). In contrast, neither *LysM*-Cre+, *CaMKII*-Cre+, nor *LysM*-Cre+:*CaMKII*-Cre + mice exhibited lipofuscinosis relative to Cre– littermates (B–D, RM ANOVA effect of *CaMKII*-Cre, $p = .831$, effect of *LysM*-Cre, $p = .513$, *CaMKII*-Cre x *LysM*-Cre interaction, $p = .549$, n = 5–10 mice per group) at 22–24 months of age. $Grn^{-/-}$ mice also exhibited elevated SCMAS (E–H, RM ANOVA effect of genotype, $p < .0001$, n = 5–6 mice per group), a protein component of lipofuscin, while *LysM*-Cre +, *CaMKII*-Cre+, and *LysM*-Cre+:*CaMKII*-Cre + mice did not (E–H, RM ANOVA effect of *CaMKII*-Cre, $p = .093$, effect of *LysM*-Cre, $p = .184$, *CaMKII*-Cre x *LysM*-Cre interaction, $p = .414$, n = 4–10 mice per group). Scale bars represent 50 μm. VPM/VPL = ventroposteromedial/ventroposterolateral thalamus. ** = $p < .01$, *** = $p < .001$, and **** = $p < .0001$ by *t*-test.

or *CaMKII*-Cre, either alone or in combination, on GFAP (Fig. 5B–D) or CD68 immunoreactivity (Fig. 5F–H). Taken together with the lipofuscin results described above, these data show that microglial progranulin reduction is not sufficient to produce lipofuscinosis and gliosis in neuronal progranulin-insufficient mice, even at advanced ages.

3.6. Reduction of microglial progranulin does not exacerbate behavioral deficits in neuronal progranulin-deficient mice

While aging mice for assessment of pathology, we also measured several FTD-relevant behaviors that are disrupted by progranulin insufficiency in mice. Both global $Grn^{-/-}$ and *Cx3Cr1*-Cre + microglial progranulin-deficient mice develop an elevated grooming phenotype that may model compulsive behavior in FTD (Lui et al., 2016; Krabbe et al., 2017). We therefore assessed grooming behavior at ages 12, 15, and 18 months in Cre–, *LysM*-Cre+, *CaMKII*-Cre+, and *LysM*-Cre +:*CaMKII*-Cre+ littermates (Fig. 6A), and observed observed increased grooming in *LysM*-Cre+ microglial progranulin-insufficient mice. Neither *CaMKII*-Cre+ neuronal progranulin-insufficient mice nor *LysM*-Cre +:*CaMKII*-Cre+ mice exhibited significantly increased grooming.

We and others have previously reported social deficits in $Grn^{+/-}$, $Grn^{-/-}$, and *CaMKII*-Cre+ neuronal progranulin-insufficient mice (Kayasuga et al., 2007; Yin et al., 2010b; Ghoshal et al., 2012; Filiano et al., 2013; Arrant et al., 2016; Arrant et al., 2017). Additionally, $Grn^{-/-}$ mice and *Cx3Cr1*-Cre+ microglial progranulin-insufficient mice develop an elevated grooming phenotype that may model compulsive behavior in FTD (Lui et al., 2016; Krabbe et al., 2017). We therefore assessed social behavior in Cre–, *LysM*-Cre+, *CaMKII*-Cre+, and *LysM*-Cre+:*CaMKII*-Cre+ littermates. At age 18–21 months, we observed social deficits in *CaMKII*-Cre+ neuronal progranulin-insufficient mice in the three-chamber sociability test (Fig. 6B), with a trend for deficits in *LysM*-Cre+ microglial progranulin-insufficient mice. *LysM*-Cre+:*CaMKII*-Cre+ mice exhibited normal sociability.

The presence of behavioral deficits in *CaMKII*-Cre+ and *LysM*-Cre+ mice, but not *LysM*-Cre+:*CaMKII*-Cre+ mice was surprising, and potentially indicated that selective reduction of progranulin from both neurons and microglia was masking the effects of reduction from a single cell type. To test for this possibility, we assessed *LysM*-Cre +:*CaMKII*-Cre+ mice in the tube test for social dominance. We have previously reported that reduction of neuronal progranulin with *CaMKII*-Cre and *Nestin*-Cre causes a low dominance phenotype in this test (Arrant et al., 2017), and observed no significant phenotype in this test in *LysM*-Cre+ mice (Fig. 2D). When tested at around 21 months of age, we observed a robust decrease in social dominance in *LysM*-Cre +:*CaMKII*-Cre+ mice, similar to that in *CaMKII*-Cre + mice, showing that microglial progranulin reduction did not somehow mask the

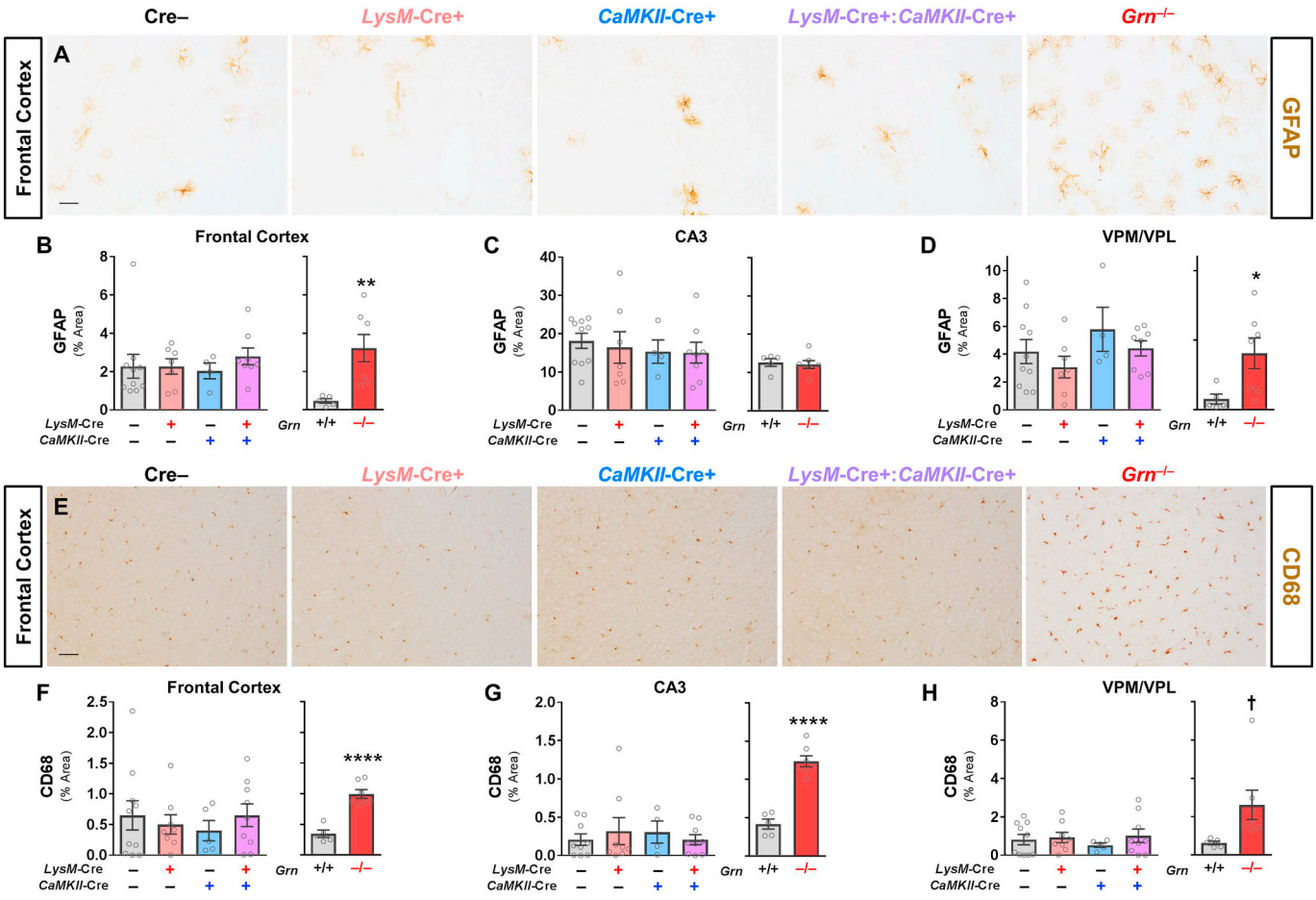

Fig. 5. Microglial Progranulin Reduction Does Not Produce Gliosis in *CaMKII*-Cre Neuronal Progranulin-insufficient Mice.
Brains from 7–10 month-old *Grn*$^{-/-}$ mice exhibited gliosis, with significant elevation of both GFAP (A–D, RM ANOVA genotype x region interaction, $p = .0487$, n = 5–7 mice per group) and CD68 (E–H, RM ANOVA effect of genotype, $p = .0087$, n = 5–7 mice per group). 22–24 month-old *LysM*-Cre+, *CaMKII*-Cre+, or *LysM*-Cre+:*CaMKII*-Cre + mice did not exhibit elevated GFAP (A–D, RM ANOVA effect of *CaMKII*-Cre, $p = .889$, effect of *LysM*-Cre, $p = .588$, *CaMKII*-Cre x *LysM*-Cre interaction, $p = .773$, n = 4–10 mice per group) or CD68 (E–H, RM ANOVA effect of *CaMKII*-Cre, $p = .974$, effect of *LysM*-Cre, $p = .584$, *CaMKII*-Cre x *LysM*-Cre interaction, $p = .805$, n = 4–10 mice per group). Scale bars represent 50 μm. VPM/VPL = ventroposteromedial/ventroposterolateral thalamus. * = $p < .05$ and ** = $p < .01$ by *t*-test.

behavioral effects of neuronal progranulin reduction.

These data show that microglial progranulin reduction does not exacerbate the behavioral deficits of neuronal progranulin-insufficient mice, and suggest that neuronal and microglial progranulin deficiency may underlie distinct behaviors in global progranulin-insufficient mice.

4. Discussion

This study shows that *LysM*-Cre-mediated microglial progranulin reduction does not further reduce total brain progranulin, induce lipofuscinosis and gliosis, or exacerbate behavioral deficits in *CaMKII*-Cre + neuronal progranulin-insufficient mice. Because these Cre transgenes were expressed in *Grn*$^{fl/fl}$ mice, many neurons and microglia targeted by each Cre exhibited almost no detectable progranulin immunolabeling (see Figs. 1 and 3 and (Arrant et al., 2017)). The lack of lipofuscinosis in progranulin-deficient neurons and lack of microgliosis from progranulin-deficient microglia provides insight into the development of pathology due to progranulin insufficiency. Additionally, the differential effects of *LysM*-Cre and *CaMKII*-Cre on behavior add to a growing literature on mechanisms underlying the development of behavioral deficits in progranulin-insufficient mice.

The failure of *LysM*-Cre to reduce total brain progranulin levels is somewhat surprising given the clear reduction in microglial progranulin immunoreactivity (Fig. 1A, B) and reports that *LysM*-Cre reduces microglial progranulin RNA levels by > 50% in *Grn*$^{fl/fl}$ mice (Minami et al., 2014; Petkau et al., 2017b). We found that roughly 1/3 of microglia maintained some degree of progranulin immunolabeling in *LysM*-Cre+ mice, and it seems that these microglia expressed enough progranulin to prevent a reduction in total brain progranulin levels. Microglia do produce measurable brain progranulin, as expression of *Cx3Cr1*-Cre, which nearly completely depletes microglial progranulin, reduces brain progranulin protein by around 30% in *Grn*$^{fl/fl}$ mice (Krabbe et al., 2017).

The effects of *LysM*-Cre and *Cx3Cr1*-Cre on brain progranulin levels stand in contrast to the stronger effects of neuronal progranulin depletion with *CaMKII*-Cre, which reduces progranulin protein in the cortex by 40–50% (Fig. 3F and (Arrant et al., 2017)), or *Nestin*-Cre, which reduces progranulin protein throughout the brain by 50% or more (Arrant et al., 2017; Petkau et al., 2017a). These studies indicate that at least half of total brain progranulin is produced by neurons, with microglia contributing most of the rest. An important caveat to this conclusion is that microglial progranulin expression appears to be more dynamic than neuronal progranulin expression. Microglia strongly increase progranulin expression in response to injury (Moisse et al., 2009; Naphade et al., 2010; Petkau et al., 2010; Tanaka et al., 2013), while neuronal progranulin appears relatively static, though physical exercise may modestly increase neuronal progranulin expression in the hippocampus (Asakura et al., 2011; Arrant et al., 2015).

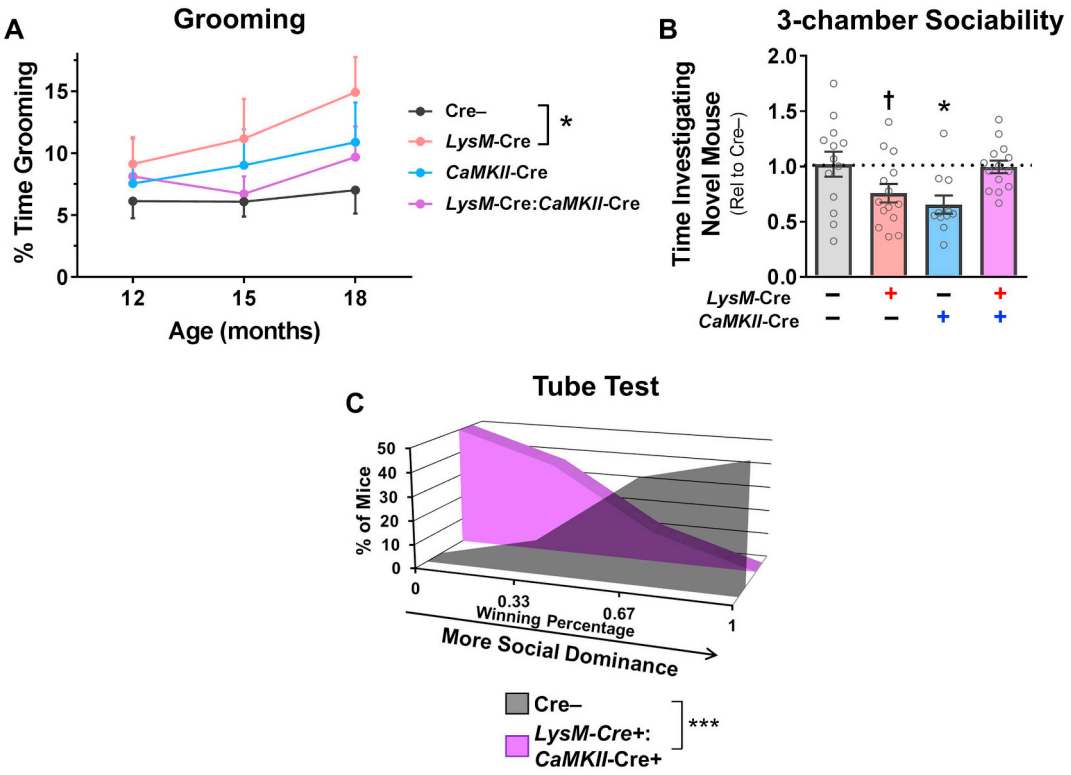

Fig. 6. Microglial Progranulin Reduction Does Not Exacerbate Behavioral Deficits in *CaMKII*-Cre Neuronal Progranulin-insufficient Mice.
LysM-Cre + microglial progranulin-insufficient mice exhibited elevated grooming behavior from ages 12–18 months (A, * = RM ANOVA effect of genotype, $p = .0375$, $n = 13–16$ mice per group), but neither *CaMKII*-Cre + neuronal progranulin-insufficient mice or *LysM*-Cre + :*CaMKII*-Cre + mice exhibited elevated grooming. At 18–21 months of age, *CaMKII*-Cre + neuronal progranulin-insufficient mice exhibited impaired social investigation in the three-chamber sociability test (B, ANOVA *CaMKII*-Cre x *LysM*-Cre interaction, $p = .0010$, $n = 11–14$ mice per group). *LysM*-Cre + microglial progranulin-insufficient mice also exhibited a trend for impaired sociability ($p = .0835$ by Dunnett's post-hoc test). *LysM*-Cre + :*CaMKII*-Cre + mice exhibited no social deficits. Despite the lack of sociability or grooming phenotypes, *LysM*-Cre + :*CaMKII*-Cre + mice had a low-dominance phenotype in the tube test at age 21 months (C, Mann-Whitney test, $p = .0004$, n = 8–10 mice per group). † = $p < .1$ by Dunnett's post-hoc test, * = $p < .05$ by Dunnett's post-hoc test, and *** = $p < .001$ by Mann-Whitney test.

The lack of pathology in *LysM*-Cre + :*CaMKII*-Cre + mice, despite the apparent progranulin deficiency of many neurons and microglia (Figs. 1 and 3), shows that progranulin from extracellular sources can prevent severe lysosomal dysfunction and lipofuscin accumulation in progranulin-deficient cells. The residual progranulin in *LysM*-Cre + :*CaMKII*-Cre + mice is likely produced by neurons and microglia not targeted by either Cre transgene. Interneurons in the cortex and hippocampus could be a significant source of residual progranulin, as *CaMKII*-Cre is expressed primarily in excitatory neurons (Tsien et al., 1996; Sik et al., 1998). Consistent with this possibility, *Nestin*-Cre, expressed by neural precursor cells (Zimmerman et al., 1994; Tronche et al., 1999), produces an even stronger reduction in cortical progranulin in $Grn^{fl/fl}$ mice than *CaMKII*-Cre (Arrant et al., 2017). Additionally, progranulin secreted from neurons in regions that do not strongly express *CaMKII*-Cre, such as the striatum or thalamus (Fig. 3E) could diffuse into the cortex or hippocampus and prevent pathology. Microglia not targeted by *LysM*-Cre could also be a significant source of the residual progranulin in *LysM*-Cre + /*CaMKII*-Cre + mice, as around 1/3 of microglia maintained detectable progranulin immunolabeling in *LysM*-Cre + mice (Fig. 1A, B). Progranulin secreted from these neurons and microglia could be taken up and processed by progranulin-deficient neurons and microglia (Hu et al., 2010; Zhou et al., 2015; Holler et al., 2017), which appears to prevent development of pathology.

It is possible that crossing mice with more robust Cre transgenes targeting microglia (e.g. *Cx3Cr1*-Cre (Krabbe et al., 2017)) or neurons (e.g. *Nestin*-Cre (Arrant et al., 2017; Petkau et al., 2017a)) would more strongly reduce total brain progranulin and potentially cause lipofuscinosis and gliosis. However, even complete depletion of neuronal and microglial progranulin may not be sufficient to induce pathology in mice, as peripheral immune cells can infiltrate the brain, express progranulin, and improve gliosis in $Grn^{-/-}$ mice (Yang et al., 2014).

Despite the lack of lipofuscinosis and gliosis, we and others have reported that selective reduction of neuronal (Arrant et al., 2017) and microglial (Lui et al., 2016; Krabbe et al., 2017) progranulin induces behavioral deficits. Reduction of both neuronal and microglial progranulin induces social deficits in the three-chamber sociability test (Fig. 6) (Arrant et al., 2017; Krabbe et al., 2017), and at least trends for impaired amygdala activation in a novel, social environment (Fig. 2) (Arrant et al., 2017). However, reduction of neuronal and microglial progranulin also produces distinct behavioral effects. Reduction of neuronal progranulin with *CaMKII*-Cre or *Nestin*-Cre produces social dominance deficits (Arrant et al., 2017), while reduction of microglial progranulin with *LysM*-Cre does not (Fig. 2). Reduction of microglial progranulin with *Cx3Cr1*-Cre (Krabbe et al., 2017) and *LysM*-Cre (Fig. 6) elevates grooming, while reduction of neuronal progranulin has a weaker, statistically non-significant, effect (Fig. 6).

The presence of these behavioral phenotypes in the absence of clear lipofuscinosis or gliosis in cell-type-specific progranulin-insufficient mice and global $Grn^{+/-}$ mice (Filiano et al., 2013) shows that lipofuscinosis and gliosis do not cause these behavioral deficits. Instead, the partially divergent behavioral phenotypes of neuronal and microglial progranulin-insufficient mice raises the possibility that distinct mechanisms mediated primarily by neurons or microglia may underlie social dominance deficits and elevated grooming. We have associated altered neuronal morphology with social dominance changes in global $Grn^{+/-}$ mice (Arrant et al., 2016), while elevated grooming and food burrowing in global $Grn^{-/-}$ may be due to increased inflammation in the brain (Minami et al., 2015; Lui et al., 2016; Krabbe et al., 2017).

Collectively, these studies show that neuronal progranulin appears to be important for social dominance behaviors, microglial progranulin appears to be important for compulsive behaviors, and both appear to be important for social investigation.

Given the lack of effect of *LysM*-Cre on total brain progranulin, it was unsurprising that *LysM*-Cre did not worsen the behavioral phenotypes of *CaMKII*-Cre+ neuronal progranulin-insufficient mice. However, it was somewhat surprising to observe that, if anything, *LysM*-Cre+:*CaMKII*-Cre+ mice had less of a behavioral phenotype than mice expressing a single Cre transgene. We are uncertain of the mechanism for this apparent protection, as mice with global progranulin insufficiency exhibit both impaired sociability (Yin et al., 2010b; Filiano et al., 2013) and elevated grooming (Lui et al., 2016; Krabbe et al., 2017). However, the presence of a robust social dominance phenotype in *LysM*-Cre+:*CaMKII*-Cre+ mice (Fig. 6C) shows that expression of both Cre transgenes did not somehow rescue all behavioral phenotypes of *CaMKII*-Cre neuronal progranulin-insufficient mice.

In summary, this study provides evidence that extracellular progranulin is sufficient to prevent lipofuscinosis in progranulin-deficient neurons and microgliosis from progranulin-deficient microglia. However, this residual, extracellular progranulin is not sufficient to rescue behavioral deficits caused by progranulin deficiency in neurons or microglia. The effects of progranulin insufficiency on neurons and microglia may underlie distinct behavioral changes, with microglial progranulin insufficiency appearing to have a particularly strong effect on compulsive behaviors. Further study of the role of impaired neuronal and microglial function in FTD due to *GRN* mutations may lead to novel therapeutic targets and provide broader insight into the pathogenesis of FTD with TDP-43 pathology.

Acknowledgements

We thank Miriam Roberson and James Black for help with mouse breeding and colony management, Jeremy Herskowitz for assistance with confocal imaging, and Robert Farese, Jr. for providing $Grn^{fl/fl}$ mice. This study was funded by the Consortium for Frontotemporal Dementia Research and the Bluefield Project to Cure FTD, a Ruth L. Kirschstein National Research Service Award Fellowship (F32NS090678), a Glenn/AFAR postdoctoral fellowship from the American Federation for Aging Research, the National Institute of Neurological Disorders and Stroke (R01NS075487, P30NS47466), and the National Institute on Aging (K99AG056597). Behavioral studies were performed in the Evelyn F. McKnight Brain Institute Behavioral Assessment Core at the University of Alabama at Birmingham.

References

Abram, C.L., et al., 2014. Comparative analysis of the efficiency and specificity of myeloid-Cre deleting strains using ROSA-EYFP reporter mice. J. Immunol. Methods 408, 89–100.
Ahmed, Z., et al., 2010. Accelerated lipofuscinosis and ubiquitination in granulin knockout mice suggest a role for progranulin in successful aging. Am. J. Pathol. 177, 311–324.
Almeida, M.R., et al., 2016. Portuguese family with the co-occurrence of frontotemporal lobar degeneration and neuronal ceroid lipofuscinosis phenotypes due to progranulin gene mutation. Neurobiol. Aging 41 (200), e1–e5.
Arrant, A.E., et al., 2015. Effects of exercise on progranulin levels and gliosis in progranulin-insufficient mice. eNeuro 2.
Arrant, A.E., et al., 2016. Progranulin haploinsufficiency causes biphasic social dominance abnormalities in the tube test. Genes Brain Behav. 15, 588–603.
Arrant, A.E., et al., 2017. Restoring neuronal progranulin reverses deficits in a mouse model of frontotemporal dementia. Brain 140, 1447–1465.
Arrant, A.E., et al., 2018. Partial Tmem106b reduction does not correct abnormalities due to progranulin haploinsufficiency. Mol. Neurodegener. 13, 32.
Asakura, R., et al., 2011. Involvement of progranulin in the enhancement of hippocampal neurogenesis by voluntary exercise. Neuroreport 22, 881–886.
Baker, M., et al., 2006. Mutations in progranulin cause tau-negative frontotemporal dementia linked to chromosome 17. Nature 442, 916–919.
Beel, S., et al., 2017. Progranulin functions as a cathepsin D chaperone to stimulate axonal outgrowth in vivo. Hum. Mol. Genet. 26, 2850–2863.
Chang, M.C., et al., 2017. Progranulin deficiency causes impairment of autophagy and TDP-43 accumulation. J. Exp. Med. 214, 2611–2628.
Chitramuthu, B.P., et al., 2010. Progranulin modulates zebrafish motoneuron development in vivo and rescues truncation defects associated with knockdown of Survival motor neuron 1. Mol. Neurodegener. 5, 41.
Clausen, B.E., et al., 1999. Conditional gene targeting in macrophages and granulocytes using LysMcre mice. Transgenic Res. 8, 265–277.
Cruts, M., et al., 2006. Null mutations in progranulin cause ubiquitin-positive frontotemporal dementia linked to chromosome 17q21. Nature 442, 920–924.
De Muynck, L., et al., 2013. The neurotrophic properties of progranulin depend on the granulin E domain but do not require sortilin binding. Neurobiol. Aging 34, 2541–2547.
Evers, B.M., et al., 2017. Lipidomic and transcriptomic basis of lysosomal dysfunction in progranulin deficiency. Cell Rep. 20, 2565–2574.
Filiano, A.J., et al., 2013. Dissociation of frontotemporal dementia–related deficits and neuroinflammation in progranulin haploinsufficient mice. J. Neurosci. 33, 5352–5361.
Gass, J., et al., 2006. Mutations in progranulin are a major cause of ubiquitin-positive frontotemporal lobar degeneration. Hum. Mol. Genet. 15, 2988–3001.
Gass, J., et al., 2012. Progranulin regulates neuronal outgrowth independent of sortilin. Mol. Neurodegener. 7, 33.
Ghoshal, N., et al., 2012. Core features of frontotemporal dementia recapitulated in progranulin knockout mice. Neurobiol. Dis. 45, 395–408.
Hall, N.A., et al., 1991. Lysosomal storage of subunit c of mitochondrial ATP synthase in Batten's disease (ceroid-lipofuscinosis). Biochem. J. 275, 269–272 Pt 1.
Holler, C.J., et al., 2017. Intracellular proteolysis of progranulin generates stable, lysosomal granulins that are haploinsufficient in patients with frontotemporal dementia caused by GRN mutations. eNeuro 4.
Hu, F., et al., 2010. Sortilin-mediated endocytosis determines levels of the frontotemporal dementia protein, progranulin. Neuron 68, 654–667.
Jackman, K., et al., 2013. Progranulin deficiency promotes post-ischemic blood-brain barrier disruption. J. Neurosci. 33, 19579–19589.
Jian, J., et al., 2016. Progranulin recruits HSP70 to beta-glucocerebrosidase and is therapeutic against gaucher disease. EBioMedicine 13, 212–224.
Kayasuga, Y., et al., 2007. Alteration of behavioural phenotype in mice by targeted disruption of the progranulin gene. Behav. Brain Res. 185, 110–118.
Klein, Z. A., et al., 2017. Loss of TMEM106B ameliorates lysosomal and frontotemporal dementia-related phenotypes in progranulin-deficient mice. Neuron 95, 281–296 e6.
Kominami, E., et al., 1992. Specific storage of subunit c of mitochondrial ATP synthase in lysosomes of neuronal ceroid lipofuscinosis (Batten's disease). J. Biochem. 111, 278–282.
Krabbe, G., et al., 2017. Microglial NFkappaB-TNFalpha hyperactivation induces obsessive-compulsive behavior in mouse models of progranulin-deficient frontotemporal dementia. Proc. Natl. Acad. Sci. U. S. A. 114, 5029–5034.
Longhena, F., et al., 2017. Depletion of progranulin reduces GluN2B-containing NMDA receptor density, tau phosphorylation, and dendritic arborization in mouse primary cortical neurons. J. Pharmacol. Exp. Ther. 363, 164–175.
Lui, H., et al., 2016. Progranulin deficiency promotes circuit-specific synaptic pruning by microglia via complement activation. Cell 165, 921–935.
Martens, L.H., et al., 2012. Progranulin deficiency promotes neuroinflammation and neuron loss following toxin-induced injury. J. Clin. Invest. 122, 3955–3959.
Minami, S.S., et al., 2014. Progranulin protects against amyloid β deposition and toxicity in Alzheimer's disease mouse models. Nat. Med. 20, 1157–1164.
Minami, S.S., et al., 2015. Reducing inflammation and rescuing FTD-related behavioral deficits in progranulin-deficient mice with alpha7 nicotinic acetylcholine receptor agonists. Biochem. Pharmacol. 97, 454–462.
Moisse, K., et al., 2009. Divergent patterns of cytosolic TDP-43 and neuronal progranulin expression following axotomy: implications for TDP-43 in the physiological response to neuronal injury. Brain Res. 1249, 202–211.
Naphade, S.B., et al., 2010. Progranulin expression is upregulated after spinal contusion in mice. Acta Neuropathol. 119, 123–133.
Palop, J.J., et al., 2011. Quantifying biomarkers of cognitive dysfunction and neuronal network hyperexcitability in mouse models of Alzheimer's disease: depletion of calcium-dependent proteins and inhibitory hippocampal remodeling. In: Roberson, E.D. (Ed.), Alzheimer's Disease and Frontotemporal Dementia: Methods and Protocols. Humana Press, Totowa, NJ, pp. 245–262.
Petkau, T.L., et al., 2010. Progranulin expression in the developing and adult murine brain. J. Comp. Neurol. 518, 3931–3947.
Petkau, T.L., et al., 2017a. Conditional loss of progranulin in neurons is not sufficient to cause neuronal ceroid lipofuscinosis-like neuropathology in mice. Neurobiol. Dis. 106, 14–22.
Petkau, T.L., et al., 2017b. Selective depletion of microglial progranulin in mice is not sufficient to cause neuronal ceroid lipofuscinosis or neuroinflammation. J. Neuroinflammation 14, 225.
Pinarbasi, E.S., et al., 2018. Pathogenic signal sequence mutations in progranulin disrupt SRP interactions required for mRNA stability. Cell Rep. 23, 2844–2851.
Ryan, C.L., et al., 2009. Progranulin is expressed within motor neurons and promotes neuronal cell survival. BMC Neurosci. 10, 130.
Scearce-Levie, K., et al., 2008. Abnormal social behaviors in mice lacking Fgf17. Genes Brain Behav. 7, 344–354.
Shankaran, S.S., et al., 2008. Missense mutations in the progranulin gene linked to frontotemporal lobar degeneration with ubiquitin-immunoreactive inclusions reduce progranulin production and secretion. J. Biol. Chem. 283, 1744–1753.
Sik, A., et al., 1998. The absence of a major Ca2+ signaling pathway in GABAergic neurons of the hippocampus. Proc. Natl. Acad. Sci. U. S. A. 95, 3245–3250.
Smith, K.R., et al., 2012. Strikingly different clinicopathological phenotypes determined by progranulin-mutation dosage. Am. J. Hum. Genet. 90, 1102–1107.

Tanaka, Y., et al., 2013. Increased lysosomal biogenesis in activated microglia and exacerbated neuronal damage after traumatic brain injury in progranulin-deficient mice. Neuroscience 250, 8–19.
Tanaka, Y., et al., 2014. Possible involvement of lysosomal dysfunction in pathological changes of the brain in aged progranulin-deficient mice. Acta Neuropathol. Commun. 2, 78.
Tronche, F., et al., 1999. Disruption of the glucocorticoid receptor gene in the nervous system results in reduced anxiety. Nat. Genet. 23, 99–103.
Tsien, J.Z., et al., 1996. Subregion- and cell type-restricted gene knockout in mouse brain. Cell 87, 1317–1326.
Valdez, C., et al., 2017. Progranulin-mediated deficiency of cathepsin D results in FTD and NCL-like phenotypes in neurons derived from FTD patients. Hum. Mol. Genet. 26, 4861–4872.
Van Damme, P., et al., 2008. Progranulin functions as a neurotrophic factor to regulate neurite outgrowth and enhance neuronal survival. J. Cell Biol. 181, 37–41.
Wang, J., et al., 2010. Pathogenic cysteine mutations affect progranulin function and production of mature granulins. J. Neurochem. 112, 1305–1315.
Ward, M.E., et al., 2017. Individuals with progranulin haploinsufficiency exhibit features of neuronal ceroid lipofuscinosis. Sci. Transl. Med. 9.
Warmus, B.A., et al., 2014. Tau-mediated NMDA receptor impairment underlies dysfunction of a selectively vulnerable network in a mouse model of frontotemporal dementia. J. Neurosci. 34, 16482–16495.
Wils, H., et al., 2012. Cellular ageing, increased mortality and FTLD-TDP-associated neuropathology in progranulin knockout mice. J. Pathol. 228, 67–76.
Yang, Y., et al., 2014. Wild-type bone marrow transplant partially reverses neuroinflammation in progranulin-deficient mice. Lab. Investig. 94, 1224–1236.
Yin, F., et al., 2010a. Exaggerated inflammation, impaired host defense, and neuropathology in progranulin-deficient mice. J. Exp. Med. 207, 117–128.
Yin, F., et al., 2010b. Behavioral deficits and progressive neuropathology in progranulin-deficient mice: a mouse model of frontotemporal dementia. FASEB J. 24, 4639–4647.
Zhou, X., et al., 2015. Prosaposin facilitates sortilin-independent lysosomal trafficking of progranulin. J. Cell Biol. 210, 991–1002.
Zhou, X., et al., 2017. Regulation of cathepsin D activity by the FTLD protein progranulin. Acta Neuropathol. 134, 151–153.
Zimmerman, L., et al., 1994. Independent regulatory elements in the nestin gene direct transgene expression to neural stem cells or muscle precursors. Neuron 12, 11–24.